Section A-Research paper
ISSN 2063-5346

Synthesis of Titania-ZnO Nanocomposites ofdiverse morphology for DSSC Applications

H A Deepa[1*]
Assistant Professor
Department of Chemical Engineering
Dayananda Sagar College of Engineering
Bengaluru, India
deepaha@gmail.com

G M Madhu[2]
Professor, Department of ChemicalEngineering
Ramaiah Institute of Technology
Bengaluru, India
gmmadhu@gmail.com

Ravishankar R[3]
Professor, Department of ChemicalEngineering
Dayananda Sagar College of Engineering
Bengaluru, India
ravishankar70@gmail.com

Somharsh Patel[4]
Department of Chemical Engineering
Dayananda Sagar College of Engineering
Bengaluru, India
somharsh09@gmail.com

Eldho Manoj[4]
Department of Chemical Engineering
Dayananda Sagar College of Engineering
Bengaluru, India
eldhosmanoj@gmail.com

Corresponding author: H A Deepa deepaha@gmail.com

***Abstract*—Nanocomposites of Titania-ZnO with molar ratios 2:1(TZ-S1) and 3:1(TZ-S2) were synthesized by employing a modified sol-gel method. The prepared nanocomposites were characterized employing X-ray diffraction (XRD), scanning electron microscopy (SEM), energy dispersive X-ray analysis (EDAX), UV, and BET analysis. The crystallinity and morphology of the nanostructures were compared for varying molar concentrations. The nanostructures thus synthesized were employed as photo-anode semiconductor materials in the fabrication of Dye-Sensitized Solar Cells (DSSC). The DSSC developed with the photo-anode of Titania-ZnO with a molar ratio of 3:1 exhibited better photovoltaic performance with an efficiency of 0.77% and a current density of 3.89 mA/cm^2 than the device with nanocomposites of TiO_2-ZnO with molar ratio 2:1.**

Keywords: Diverse morphology, Nanocomposite flowers, photo-anode, Titania-ZnO, photovoltaic performance, DSSC

I. Introduction

Energy has an ambiguous status appearing as a driving force that inflicts a vital change in the social aspect. Energy is a quantitative property that is embedded into the matrix of society. The Earth receives approximately 10^{11} kilowatts of solar radiation annually, while the total global energy consumption in a single calendar year stands at 15×10^{10} kilowatts. The world is in a critical situation, with 14×10^{10} kilowatts of energy being consumed by seven billion individuals. This energy demand is anticipated to increase by more than 170% over the next forty years [1, 2].

The most important highlight of renewable energy is its abundance, as it is present in immeasurable quantities. Renewable energy sources are green energy sources with a lower environmental footprint than conventional fossil fuel technology. Renewable sources have accounted for over half of the total electricity in the last decade [3-6]. The most efficient method to obtain electricity is by converting quantum energy utilizing the solar cell. There are a set of three generations of solar cells, namely, the first-generation (1G), second-generation (2G), and third-generation (3G).

Dye-sensitized solar cells (DSSCs) are an efficient substitute for conventional silicon-based

solar cells and are widely contemplated as a potential contender in the third generation of solar cells. A DSSC is made up of a photo-anode, a counter electrode, and an electrolyte sandwiched between two electrodes. The setup effectuates electricity from light without enduring any long-term chemical transformation [7-12]. The DSSC has been in the spotlight owing to its cost-effectiveness and exemplary efficiency. The solar-to-electricity conversion efficiency (η), in addition to the long-term stability, are essential parameters influencing DSSC performance.

Numerous modi operandi are currently being explored to ameliorate the theoretical photoelectric conversion efficiency of DSSCs, giving rise to an era consisting of various novel dyes inclusive of organic as well as natural dyes that help in extending the solar irradiation absorption to regions such as the infrared and near-infrared [13-16]. A DSSC's key parameters include the photo-anode, photosensitizer, and counter electrode. The overall conversion efficiency (η) of a DSSC is determined by the photocurrent density (J_{sc}), the open-circuit potential (V_{oc}), the fill factor (FF), and the intensity of the incident light [17].

Titanium dioxide, also known as titania, is one of the most bounteous compounds present on Earth, offering an extensive list of applications. This compound is most widely used as a pigment in cosmetics products and several sensors due to its distinctive physical and chemical properties. It is also the most extensively studied wide band-gap semiconductor for photo-catalytic processes, which has caught the scientific community's attention in recent years. Titania particles with sizes lesser than 100 nm are capable of exhibiting visible light transparency as well as UV light absorption that is of a high order. However, ZnO is a photo-catalyst that is a potential substitute for TiO_2 because it has a wider bandgap, higher solar absorption, and conversion efficiency [18-28].

In this ambiguous field of Engineering, plenty of researchers have contributed toward the sole cause of innovation. For instance, Vivek Dhas et al. [29] synthesized thin anatase TiO_2 nanoleaves by the method of hydrothermal to be compared with that of TiO_2 nanoleaves synthesized Hydro-thermally using the Degussa P25 powder. Additionally, both of these samples were synthesized for the purpose of DSSCs [29]. Similarly, Hegazy et al. synthesized the TiO_2 nanoparticles at 350 ºC for a large area of DSSC to obtain an efficiency of 4.21% [30]. Apart from this, S Satyajyothi et al. fabricated the DSSC based on TiO_2 nanopowders equipping the sol-gel method of preparation. The TiO_2 nanomaterials were subjected to XRD, SEM, and DTA. The efficiency of the DSSC fabricated using the beetroot dye was found to be 1.3%, while that of the Henna dye was calculated as 1.08% [31]. In the present study, the nanocomposites of Titania-ZnO with diverse molar ratios were prepared utilizing the modified sol-gel technique. The variation in morphology and crystallinity of the nanostructures with changes in molar concentrations were analyzed. The synthesized nanostructures were employed as the semiconductor photo-anode materials in the formation of DSSCs, and their photovoltaic function was compared, evaluated, and the results are reported.

II. Experimental Section

A. Synthesis of Titania-ZnO using modified sol-gel method:

The TiO_2-ZnO composite was synthesized using modified sol-gel technique, which was acquired from the research conducted by Pugazhendhi et al. [32]. A stoichiometric proportion of zinc acetate dihydrate (2.195g) and ethanol (10 ml) was stirred for 15 minutes. A solution of TiO_2 nanoparticles was prepared by adding TiO_2 nanoparticles into 10 ml of deionized water. The resultant solution was agitated for 16 minutes and then added to the prepared $Zn(CH_3CO_2)_2 \cdot 2H_2O$ solution. Simultaneously, a measured quantity of 8g of NaOH was added to 10 ml of deionized water and agitated for 16 minutes. The NaOH solution was then introduced in a dropwise manner to the previously prepared solution of titania and $Zn(CH_3CO_2)_2 \cdot 2H_2O$ to a point where the pH reached 12. The mixed solution was agitated constantly for 360 minutes and was later aged for a duration of 1 day. Once the above operation was completed, the gel hence obtained was washed

multiple times with ethanol and water. Lastly, the solution prepared was filtered, and the precipitate was kept in a muffle furnace at 393K for 360 minutes. The powder was then calcined at 723K for 60 minutes, and the obtained product was characterized.

B. 2.2 Fabrication and assembling of DSSC

The DSSCs were fabricated employing a method that correlates to the method adopted by Chung et al. [33]. Photo-anode and counter electrodes were made using 2.2 mm thick fluorine-doped Tin Oxide (FTO) coated glass slides with 85% transmittance and with a resistivity of 7 Ω/m^2. The slides were washed with distilled water and then ultrasonicated in ethyl alcohol for about 10 minutes, followed by drying.

Utilizing the doctor blade procedure, the prepared nanocomposites were applied on the conductive side of the glass slides. The obtained photo-anodes were dried at an ambient temperature and sintered at 723K for a time period of thirty minutes. The glass substrates hence obtained were immersed in a 0.005 mol/l solution of the N719 dye for dye sensitization. The glass substrates were then allowed to rest in the dye for an entire day. Subsequent to this process, the coated nanofilms were washed with ethyl alcohol and made to dry in the air. A coating of Platisol T/SP was applied on an additional glass slide that formed the counter electrode. The glass substrate was sintered at 673K for thirty minutes and cooled to ambient temperature. The assembly involved the counter electrode being placed over the photo-anode and being mustered with a clasp. The Iodolyteelectrolyte (HI 30) was injected in the middle of the photo-anode and counter electrode by a capillary motion. The active region of the DSSC was close to 25 mm^2 [34].

III. Characterization

The morphology of the synthesized nanocomposites with diverse molar concentrations was determined using SEM (Tescan Vega 3). To study the crystallite phase of the synthesized nanomaterials, XRD with CuKa radiation accompanied by the standard JCPDS (PAN Analytical powder Xpert-3) was used. An EDAX study was effectuated to ascertain the elemental composition of the synthesized nanomaterials. UV-DRS (PerkinElmer UV WinLabLamda 900) was used to analyze the UV–VISIBLE absorption spectra of TiO2-ZnO nanocomposites.

The specific surface area of the nanomaterials was analysed using the BET analysis utilizing the QuantachromeNovaWin (version 11.05) instrument. The DSSC fabricated was subjected to a solar simulator with irradiation of 1000 W/m^2 along with a Keithley 2400 source meter that was operated using a computer to carry out the I-V characterization. The photo-electrical conversion efficiency (η) of the fabricated DSSC was calculated using the equation (1)

$$\eta = \frac{j_{sc}.V_{oc}.FF}{P_{in}} \quad \text{-------- (1)}$$

Where, Jsc indicates the short circuit current density, Voc is the open circuit voltage, Pin is the incident power input, and FF is the fill factor.

IV. Results and discussion

A. XRD-Analysis

The XRD pattern of TZ-S1 (2:1) and TZ-S2 (3:1) is depicted in Figure 1. The XRD pattern displayed in Figure 1 (a) affirmed the development of TZ-S1 (2:1) with the development of diffraction peaks of TiO_2 at angles of 2θ = 25.28, 38.38, 47.99, 54.15, 55.02, and 70.19 relating to the standard peaks (101), (112), (200), (105), (211), and (220), respectively of the JCPDS card # 84-1286. The development of diffraction peaks of ZnO took place at angles of 2θ =31.74, 27.42, 36.19, 47.99, 56.57, and 67.92, respectively, relating to the standard peaks (100), (002), (101), (102), (110), and (103) of the JCPDS card # 36-1451.

In addition to this, the XRD pattern displayed in Figure 1(b) reflected the development of TZ-S2 (3:1) with the development of diffraction peaks of TiO_2 at angles of 2θ = 26.01, 37.97, 48.25, 54.59, 56.57, 62.2, 67.94, and 69.09 correlating to the standard peaks (101), (112), (200), (105), (211), (204), (116),

and (220), respectively, of the JCPDS card #84-1286. The development of diffraction peaks of ZnO took place at angles of 2θ = 31.76, 34.45, 36.25, 47.55, 56.57, 63.80, 67.94, and 69.09, respectively, correlating to the standard peaks (100), (002), (101), (102), (110), (103), (112) and (201) of the JCPDS card #36-1451 [35].

Scherrer's condition was utilized to assess the crystallite size of the synthesized nanopowders [36, 32]

$D = K\lambda/\beta cos\theta$ -------- (2)

In the above-mentioned equation (2), D stands for the average size of the particles, λ signifies the wavelength of the X-ray beam, θ represents the Bragg's Angle, β indicates the line broadening at half of the maximum possible intensity, and K corresponds to the constant whose value is equal to 0.94. Using equation (2), the average particle size of TZ-S1 2:1) and TZ-S2 (3:1) was determined to be 40 nm and 29.26 nm, respectively. The change in molar concentration resulted in varied crystallite sizes of the composites.

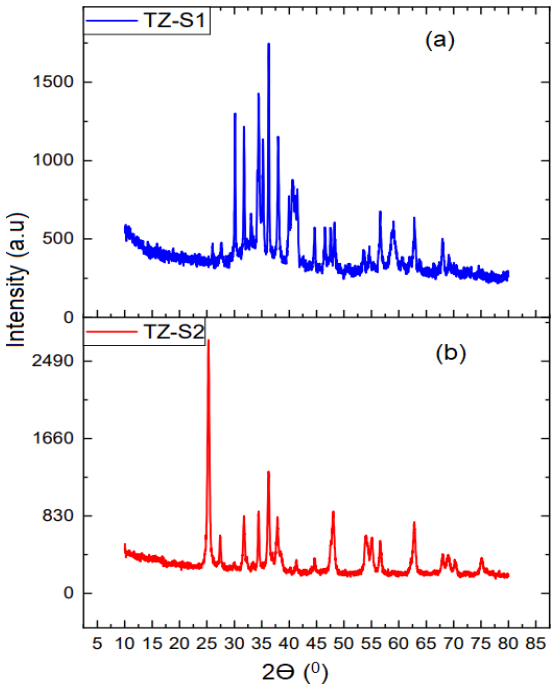

Fig. 1. XRD Analysis of a) TZ-S1 Composite (2:1) b) TZ-S2 Composite (3:1)

B. EDAX analysis

Figure 2 depicts the EDAX analysis of the synthesized nanocomposites. Based on the EDAX analysis, TiO2-ZnO (3:1) composites were formed with stoichiometric weight percentages of 33.55% Ti, 42.02% O, and 15.96% Zn. From the interpretation of the data for the above samples, the presence of carbon impurity was detected. The TiO_2-ZnO (2:1) composite was found to be in the stoichiometric weight of Ti= 9.65%, O= 53.63%, and Zn= 4.32%. Further, the EDAX analysis affirmed the presence of carbon (C) and sodium (Na) as the impurities in the TiO_2-ZnO (2:1) sample.

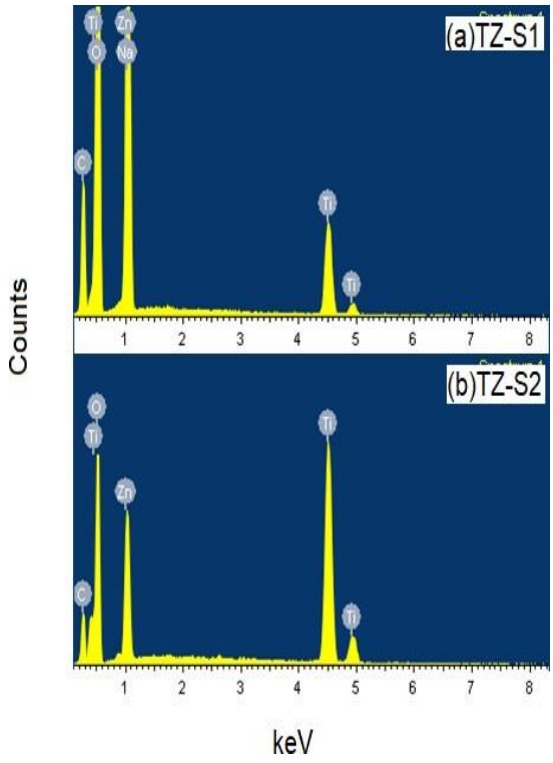

Fig. 2. EDAX Analysis of a) TZ-S1 (2:1) and b) TZ-S2 (3:1) composites

C. SEM analysis

Figure 3 displays the SEM images of TZ-S1 (2:1) and TZ-S2 (3:1). From the SEM analysis, the TZ-S2 (3:1) composites were found to be spherical in shape with agglomeration. However, the particles were found to be uniformly distributed. For the TZ-S1 (2:1)

ISSN 2063-5346

composite, the formation of the nanoflowers took place with each petal ranging in the size of 250 nm to 350 nm in diameter. In addition to this, the nanoflowers were formed in the nanometer range with an aspect ratio of 3:1 (L/D).

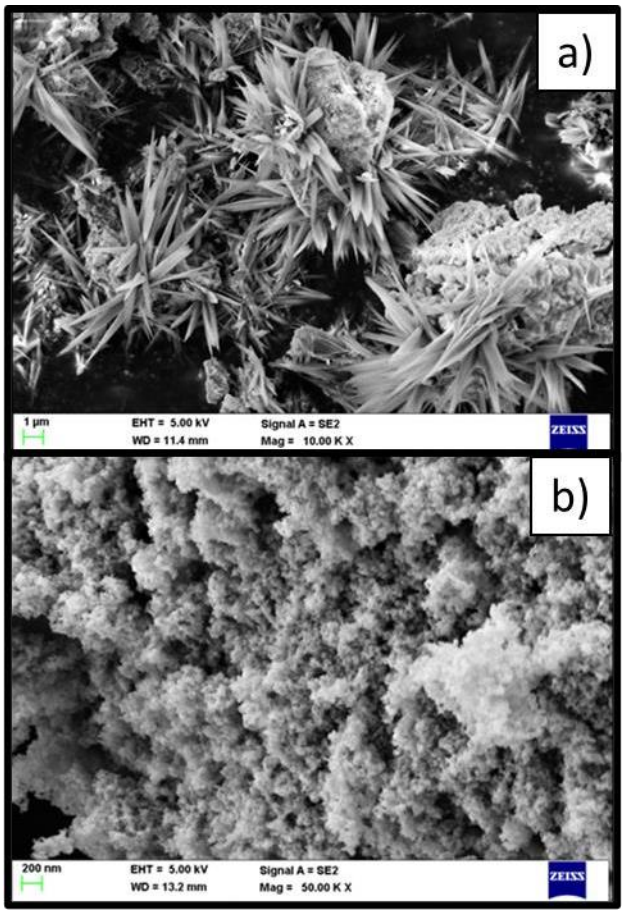

Fig. 3. SEM image of a) TZ-S1 (2:1) and b) TZ-S2 (3:1)

D. UV-analysis

The UV–Vis analysis on the synthesized Titania-ZnO composite was performed to determine the bandgap energy (E_g). From UV analysis, the E_g of the TZ-S1 (2:1) composite was determined to be 3.01 eV while that of the TZ-S2 (3:1) composite was determined to be 2.97 eV which is a slightly lower value when contrasted with that obtained by Alfanaar et al. [37]. The integration of ZnO with TiO_2 has resulted in the shifting of the cut-off wavelength (redshift) in addition to the decrease in bandgap, which could be due to the agglomeration at a larger crystallite size of the nanomaterials in the course of the synthesis process. It is important to note that the obtainment of the lower bandgap could be correlated to the presence of impurities in the samples as well as a larger crystallite size.

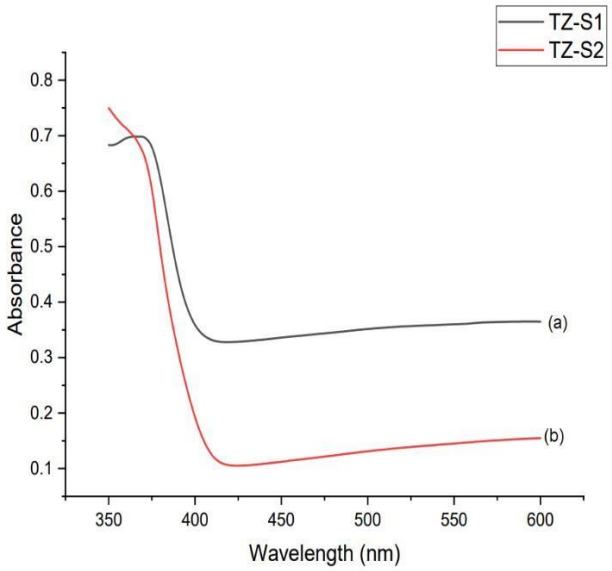

Fig. 4. UV–Vis analysis of a) TZ-S1 (2:1) and b) TZ-S2 (3:1).

E. BET analysis

The BET analysis of the composites was conducted to ascertain the specific surface area of the particles. It was learned that the surface area of the TZ-S2 (3:1) was computed to be 22.44 m^2/g while that of the TZ-S1 (2:1) was computed to be 19.33 m^2/g. Both these values were observed to be greater than those reported by Waqar Ahmad et al. [38]. In contrast to this, it was also observed that the specific area obtained by Song L et al. was much higher when compared to the results obtained for the nanocomposite samples. This might be due to the unique approach in the synthesis of the TiO_2-ZnO nanocomposite (core-shell rice grains) followed by Song L et al. using coaxial electrospinning and calcination [39]. It was observed by Jin-Kook Lee et al. that on increasing the proportion of TiO_2 in the titania paste, the surface area increased exponentially from 613 cm^2 /mg to 1070 cm^2 /mg [40]. From the above observation, we can conclude that the incorporation of nano ZnO into the TiO_2

ISSN 2063-5346

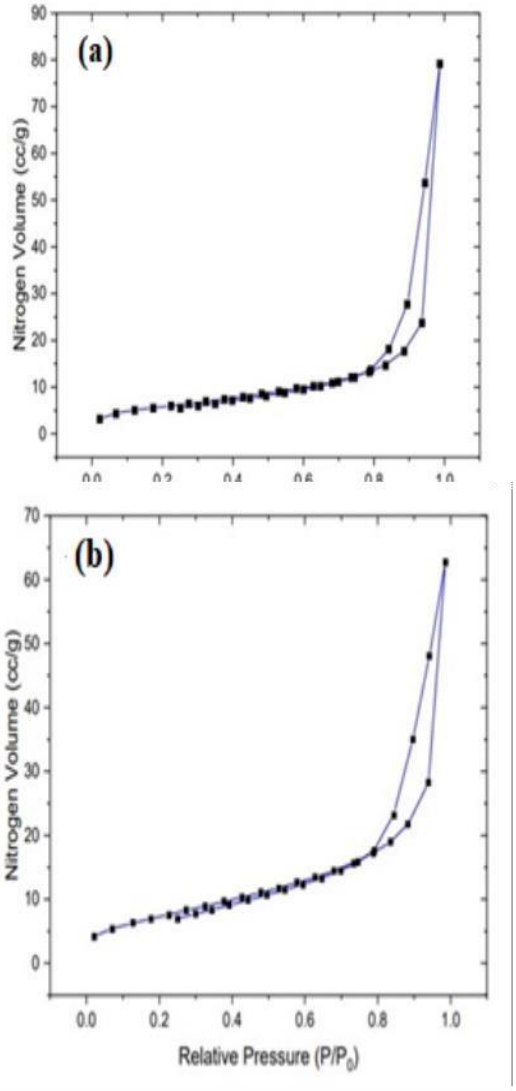

nanoparticles resulted in the decline of the specific surface area.

Fig. 5. BET Analysis of a) TiO_2-ZnO (3:1) and b) TiO_2-ZnO (2:1)

F. I-V characterization

The curve plotted between the current and voltage displayed the performance of the fabricated DSSC. Under illumination, the voltage was modified in small variations to procure the current being developed across the cell. The I-V curves of the DSSCs were generated under illumination of 100mW/cm^2 [41]. The I-V attributes of the DSSCs fabricated utilizing Titania-ZnO composite as the photo-anodes are depicted in Figure 6. From I-V characterization, we learn that the DSSC fabricated with TZ-S2 as the photo-anode exhibited a better photovoltaic performance when compared to the device with TZ-S1.

It was comprehended that the DSSC fabricated with TZ-S1 (2:1) had a V_{oc} of 0.685 V. The aforementioned value is higher when compared to that reported by Lilis Retnaningsih et al. It is worth noting that Lilis Retnaningsih et al. used a powder type of dye (Z907) for sensitization [42]. In addition to this, the V_{oc} values are identical to the values announced by Alfanaar R et al. The TiO_2-ZnO nanocomposites were obtained by utilizing a hybrid procedure where anthocyanin pigments were obtained from Rosella flowers to be further utilized as the dye by Alfanaar R et al. [37]. The I_{sc} and η values are higher when contrasted to the quantities revealed by Manikandan et al. [43]. The difference in the V_{oc} and J_{sc} values may have been due to the agglomeration of particles of the nanocomposites which, might have effectuated the opposition for electron mobility. [44, 45]. The efficiency was found to be 0.67% which is higher than that obtained by Rahman, M.F et al. [46]. The lower efficiency may be due to the formation of a complex when nano ZnO was coupled with nano TiO_2, which might have caused hindrance to the electron mobility across the photo-anode [47].

In addition to this, the DSSC thus fabricated with TZ-S2 (3:1) was perceived to have a Voc of 0.708 V. On analogizing, it was learned that the above value was a greater one when contrasted to the value disclosed by Rheimaet al. [48]. The efficiency obtained for TZ-S2 (3:1) composite as photo-anode was 0.77%. On comparison, it was learned that this value of efficiency was a lower one when juxtaposed to that of YL Xie et al., who utilized the electrochemical method of preparation to obtain highly cataloged vertically oriented nanotubes with an unwavering number of pore sizes. It must be noted that a Ru-based N719 dye was used in the sensitization of the TiO2-ZnO nanocomposite by YL Xieet al. [49]. The short-circuit current density obtained by TZ-S2 (3:1) was 3.89 mA/cm2 which, is identical to that acquired

by LEI, F et al. [50], who had prepared the sample using the hydrothermal method. Reviewing Table 1, it was observed that the overall performance of the device fabricated with TZ-S2 composite as the photo-anode semiconductor material was better than that of the device fabricated with TZ-S1 composite with a Voc of 0.7085 V, Jsc of 3.89 mA/cm2, FF of 27.95%, and η of 0.77%.

TABLE 1. I-V CHARACTERISTICS OF DSSC FABRICATED USING TITANIA-ZNO COMPOSITES

Photo-anode	**V_{oc} (V)**	**J_{sc} (mA/cm^2)**	**FF**	**η**
TZ-S1 (2:1)	0.685	3.810	25.68%	0.67%
TZ-S2 (3:1)	0.7085	3.890	27.95%	0.77%

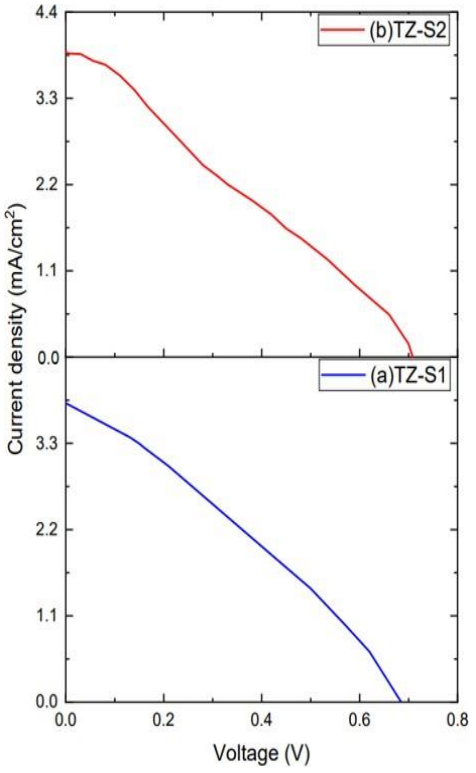

Fig. 6. I-V characteristics of DSSC fabricated with a) TZ-S1 (2:1), and b) TZ-S2 (3:1).

V. Conclusion

Through thorough study and interpretation, a suitable conclusion for the research conducted on the photovoltaic performance of solar devices synthesized using photo-anode semiconductor materials of different molar ratios could be achieved. It is important to note that the synthesis of the TiO_2-ZnO nanocomposites with different molar ratios was completed utilizing the modified sol-gel method. Variation in molar concertation resulted in diverse morphologies, such as nanocomposite flowers and nanocomposite particles for Titania-ZnO composites of 2:1 and 3:1, respectively. The photovoltaic performance of the DSSC fabricated with the 3:1 composite was found to be better than that fabricated with the 2:1 composite, which is due to the variation in specific surface area, which is the key factor for effective dye-loading on the surface of the photo-anode. Additionally, through inference, it could also be noted that the incorporation of ZnO with TiO_2 reduced the bandgap energy significantly as evident in the UV-Analysis. Through the I-V analysis, it could be concluded that the DSSC fabricated with TZ-S2 with a molar ratio of 3:1 had the better Voc, Jsc, FF, and efficiency values than that of the device fabricated with TZ-S1 sample in the ratio of 2:1. There is a scope for improving the efficacy of the cell by optimizing the molar concentrations of the metal-oxides and coupling them for DSSC applications.

VI. References:

[1] Shove, E. and Walker, G., 2014. What is energy for? Social practice and energy demand. *Theory, Culture & Society*, *31*(5), pp.41-58.

[2] Grätzel, M., 2009. Recent advances in sensitized mesoscopic solar cells. *Accounts of chemical research*, *42*(11), pp.1788-1798.

[3] Shahzad, U., 2012. The need for renewable energy sources. *energy*, *2*, pp.16-18.

[4] Moriarty, P. and Honnery, D., 2012. What is the global potential for renewable energy? *Renewable and Sustainable Energy Reviews*, *16*(1), pp.244-252.

[5] Gielen, D., Boshell, F., Saygin, D., Bazilian, M.D., Wagner, N. and Gorini, R., 2019. The role of renewable energy in the global energy transformation. *Energy Strategy Reviews*, *24*, pp.38-50.

[6] Framework, G.T., 2015. Progress toward sustainable energy.

[7] Bagher, A.M., Vahid, M.M.A. and Mohsen, M., 2015. Types of solar cells and application. *American Journal of optics and Photonics*, *3*(5), pp.94-113.

[8] Shaikh, J.S., Shaikh, N.S., Mali, S.S., Patil, J.V., Pawar, K.K., Kanjanaboos, P., Hong, C.K., Kim, J.H. and Patil, P.S., 2018. Nanoarchitectures in dye-sensitized solar cells: metal oxides, oxide perovskites and carbon-based materials. *Nanoscale*, *10*(11), pp.4987-5034.

[9] Bella, F., Nair, J.R. and Gerbaldi, C., 2013. Towards green, efficient and durable quasi-solid dye-sensitized solar cells integrated with a cellulose-based gel-polymer electrolyte optimized by a chemometric DoE approach. *RSC advances*, *3*(36), pp.15993-16001.

[10] Lin, L.Y., Lee, C.P., Vittal, R. and Ho, K.C., 2010. Selective conditions for the fabrication of a flexible dye-sensitized solar cell with Ti/TiO2 photo-anode. *Journal of Power Sources*, *195*(13), pp.4344-4349.

[11] Lee, C.P., Lin, L.Y., Tsai, K.W., Vittal, R. and Ho, K.C., 2011. Enhanced performance of dye-sensitized solar cell with thermally-treated TiN in its TiO2 film prepared at low temperature. *Journal of Power Sources*, *196*(3), pp.1632-1638.

[12] Grätzel, M., 2003. Dye-sensitized solar cells. *Journal of photochemistry and photobiology C: Photochemistry Reviews*, *4*(2), pp.145-153.

[13] Chang, W.C., Sie, S.Y., Yu, W.C., Lin, L.Y. and Yu, Y.J., 2016. Preparation of nano-composite gel electrolytes with metal oxide additives for dye-sensitized solar cells. *Electrochimica Acta*, *212*, pp.333-342.

[14] Nazeeruddin, M.K., Baranoff, E. and Grätzel, M., 2011. Dye-sensitized solar cells: A brief overview. *Solar energy*, *85*(6), pp.1172-1178.

[15] Sirimanne, P.M., 2008. Contribution of H-aggregated dye molecules in photocurrent generation of solid-state TiO2| pyrogallol red| CuI solar cell. *Renewable Energy*, *33*(6), pp.1424-1428.

[16] Pastore, M. and De Angelis, F., 2010. Aggregation of organic dyes on TiO2 in dye-sensitized solar cells models: an ab initio investigation. *ACS nano*, *4*(1), pp.556-562.

[17] Sharma, K., Sharma, V. and Sharma, S.S., 2018. Dye-sensitized solar cells: fundamentals and current status. *Nanoscale research letters*, *13*(1), pp.1-46.

[18] Chen, X. and Mao, S.S., 2007. Titanium dioxide nanomaterials: synthesis, properties, modifications, and applications. *Chemical reviews*, *107*(7), pp.2891-2959. (XRD)

[19] Chen, X., Shen, S., Guo, L. and Mao, S.S., 2010. Semiconductor-based photocatalytic hydrogen generation. *Chemical reviews*, *110*(11), pp.6503-6570.

[20] Wijnhoven, J.E. and Vos, W.L., 1998. Preparation of photonic crystals made of air spheres in titania. *Science*, *281*(5378), pp.802-804.

[21] Mekasuwandumrong, O., Pawinrat, P., Praserthdam, P. and Panpranot, J., 2010. Effects of synthesis conditions and annealing post-treatment on the photocatalytic activities of ZnO nanoparticles in the degradation of methylene blue dye. *Chemical Engineering Journal*, *164*(1), pp.77-84.

[22] Byun, K.T., Seo, K.W., Shim, I.W. and Kwak, H.Y., 2008. Syntheses of ZnO and ZnO-coated TiO2 nanoparticles in various alcohol solutions at multibubble sonoluminescence (MBSL) condition. *Chemical Engineering Journal*, *135*(3), pp.168-173.

[23] Venkatesha, T.G., Nayaka, Y.A., Viswanatha, R., Vidyasagar, C.C. and Chethana, B.K., 2012. Electrochemical synthesis and photocatalytic behavior of flower shaped ZnO microstructures. *Powder technology*, *225*, pp.232-238.

[24] Shi, R., Yang, P., Dong, X., Ma, Q. and Zhang, A., 2013. Growth of flower-like ZnO on ZnO nanorod arrays created on zinc substrate through low-temperature hydrothermal synthesis. *Applied Surface Science*, *264*, pp.162-170.

[25] Suwanboon, S., Amornpitoksuk, P., Sukolrat, A. and Muensit, N., 2013. Optical and photocatalytic properties of La-doped ZnO nanoparticles prepared via precipitation and mechanical milling method. *Ceramics International*, *39*(3), pp.2811-2819.

[26] Ma, H., Williams, P.L. and Diamond, S.A., 2013. Ecotoxicity of manufactured ZnO nanoparticles–a review. *Environmental Pollution*, *172*, pp.76-85.

[27] Xie, W., Li, Y., Shi, W., Zhao, L., Zhao, X., Fang, P., Zheng, F. and Wang, S., 2012. Novel effect of significant enhancement of gas-phase photocatalytic efficiency for nano ZnO. *Chemical engineering journal*, *213*, pp.218-224.

[28] Kim, J., Jeong, H. and Park, J.Y., 2013. Patterned horizontal growth of ZnO nanowires on SiO2 surface. *Current Applied Physics*, *13*(2), pp.425-429.

[29] Dhas, V., Muduli, S., Agarkar, S., Rana, A., Hannoyer, B., Banerjee, R. and Ogale, S., 2011. Enhanced DSSC performance with high surface area thin anatase TiO2 nanoleaves. *Solar Energy*, *85*(6), pp.1213-1219.

[30] Hegazy, A., Kinadjian, N., Sadeghimakki, B., Sivoththaman, S., Allam, N.K. and Prouzet, E., 2016. TiO2 nanoparticles optimized for photo-anodes tested in large area Dye-sensitized solar cells (DSSC). *Solar Energy Materials and Solar Cells*, *153*, pp.108-116.

[31] Sathyajothi, S., Jayavel, R. and Dhanemozhi, A.C., 2017. The fabrication of natural dye sensitized solar cell (Dssc) based on

TiO2 using henna and beetroot dye extracts. *Materials Today: Proceedings*, *4*(2), pp.668-676.

[32] Pugazhendhi, K., D'Almeida, S., Kumar, P.N., Mary, J.S.S., Tenkyong, T., Sharmila, D.J., Madhavan, J. and Shyla, J.M., 2018. Hybrid TiO2/ZnO and TiO2/Al plasmon impregnated ZnOnanocomposite photo-anodes for DSSCs: synthesis and characterisation. *Materials Research Express*, *5*(4), p.045053.

[33] Chung, S.L. and Wang, C.M., 2012. Solution combustion synthesis of TiO2 and its use for fabrication of photoelectrode for dye-sensitized solar cell. *Journal of Materials Science & Technology*, *28*(8), pp.713-722.

[34] Jongprateep, O., Puranasamriddhi, R. and Palomas, J., 2015. Nanoparticulate titanium dioxide synthesized by sol–gel and solution combustion techniques. *Ceramics International*, *41*, pp.S169-S173.

[35] Marimuthu, T. and Anandhan, N., 2017. Growth and characterization of ZnO nanostructure on TiO2-ZnO films as a light scattering layer for dye sensitized solar cells. *Materials Research Bulletin*, *95*, pp.616-624.

[36] Li, Z., Yu-Qing, F., Mao-Cong, Z., Min, W., Jia-Yu, Z., Chun-Xiang, X. and Yi-Ping, C., 2009. Performances of ZnO-based dye sensitized solar cells fabricated by hydrothermal synthesis and sol-gel technique. *Chinese Physics Letters*, *26*(1), p.018401.

[37] Alfanaar, R., Elim, P.E., Yuniati, Y., Kusuma, H.S. and Mahfud, M., 2021, February. Synthesis of TiO2/ZnO-Anthocyanin Hybrid Material for Dye Sensitized Solar Cell (DSSC). In IOP Conference Series: Materials Science and Engineering (Vol. 1053, No. 1, p. 012088). IOP Publishing.

[38] Ahmad, W., Mehmood, U., Al-Ahmed, A., Al-Sulaiman, F.A., Aslam, M.Z., Kamal, M.S. and Shawabkeh, R.A., 2016. Synthesis of zinc oxide/titanium dioxide (ZnO/TiO2) nanocomposites by wet incipient wetness impregnation method and preparation of ZnO/TiO2 paste using poly (vinylpyrrolidone) for efficient dye-sensitized solar cells. *Electrochimica Acta*, *222*, pp.473-480.

[39] Song, L., Jiang, Q., Du, P., Yang, Y., Xiong, J. and Cui, C., 2014. Novel structure of TiO2–ZnO core shell rice grain for photo-anode of dye-sensitized solar cells. *Journal of Power Sources*, *261*, pp.1-6.

[40] Lee, J.K., Jeong, B.H., Jang, S.I., Kim, Y.G., Jang, Y.W., Lee, S.B. and Kim, M.R., 2009. Preparations of TiO2 pastes and its application to light-scattering layer for dye-sensitized solar cells. *Journal of Industrial and Engineering Chemistry*, *15*(5), pp.724-729.

[41] Singh, L.K. and Koiry, B.P., 2018. Natural dyes and their effect on efficiency of TiO2 based DSSCs: a comparative study. Materials Today: Proceedings, 5(1), pp.2112-2122.

[42] Retnaningsih, L. and Muliani, L., 2016, April. The result of synthesis analysis of the powder TiO2/ZnO as a layer of electrodes for dye sensitized solar cell applications. In *AIP Conference Proceedings* (Vol. 1725, No. 1, p. 020069). AIP Publishing LLC.

[43] Manikandan, V.S., Palai, A.K., Mohanty, S. and Nayak, S.K., 2018. Eosin-Y sensitized core-shell TiO2-ZnO nano-structured photo-anodes for dye-sensitized solar cell applications. Journal of Photochemistry and Photobiology B: Biology, 183, pp.397-404.

[44] Deepa, H.A., Madhu, G.M. and Venkatesham, V., 2021. Performance evaluation of DSSC's fabricated employing TiO2 and TiO2-ZnO nanocomposite as the photo-anodes. *Materials Today: Proceedings*, *46*, pp.4579-4586.

[45] Wahyuningsih, S., Ramelan, A.H., Hidayat, R., Fadillah, G., Munawaroh, H. and Saputri, L.N.M.Z., 2017, July. Synthesis of TiO2 NRs-ZnO Composite for Dye Sensitized Solar Cell Photo-anodes. In IOP Conference Series: Earth and Environmental Science (Vol. 75, No. 1, p. 012006). IOP Publishing.

[46] Rahman, M.F., Hidayat, A. and Diantoro, M., 2020, June. The influence of TiO2 film thickness in Dye-Sensitized Solar Cells (DSSC) performance based on TiO2/Ag@ TiO2-ZnO. In Journal of Physics: Conference Series (Vol. 1572, No. 1, p. 012079). IOP Publishing.

[47] Kanmani, S.S. and Ramachandran, K., 2012. Synthesis and characterization of TiO2/ZnO core/shell nanomaterials for solar cell applications. Renewable Energy, 43, pp.149-156.

[48] Rheima, A.M., Hussain, D.H. and Abed, H.J., 2020, November. Fabrication of a new photo-sensitized solar cell using TiO2\ZnO Nanocomposite synthesized via a modified sol-gel Technique. In IOP Conference Series: Materials Science and Engineering (Vol. 928, No. 5, p. 052036). IOP Publishing.

[49] Xie, Y.L., Li, Z.X., Xu, Z.G. and Zhang, H.L., 2011. Preparation of coaxial TiO2/ZnO nanotube arrays for high-efficiency photo-energy conversion applications. Electrochemistry Communications, 13(8), pp.788-791.

[50] LEI, F., CHEN, H., SHI, Y. and XIE, J., 2013. Hydrothermal synthesis and photovoltaic properties of ZnO particles and their application in TiO2/ZnO-based dye-sensitized solar cells. Journal of the Chinese Ceramic Society, 41(1), pp.12-18.